835. Numerical modelling and validation of light gauge steel top-seat flange-cleat connection

Lee Yeong Huei[1], Tan Cher Siang[2], Mahmood Tahir[3], Shahrin Mohammad[4]
Faculty of Civil Engineering, Universiti Teknologi Malaysia, 81310 Johor Bahru, Johor, Malaysia
Email: [1]*yhlee7@live.utm.my*, [2]*tcsiang@utm.my*, [3]*mahmmodtahir@utm.my*, [4]*shahrin@utm.my*

(Received 12 July 2012; accepted 4 September 2012)

Abstract. This paper presents the numerical investigation on the moment-rotation behaviour of cold-formed top-seat flange-cleat connection, a type of light gauge steel connection which structural connection has sparked a wide range of research interest. The cold-formed channel sections were assembled back-to-back to form I-shape beam and column members. Two components were used to connect the members, notably the 2 mm cold-formed bracket and the 6 mm hot-rolled angle. The results were collected from different beam depths, namely 150 mm, 200 mm and 250 mm. The rotational stiffness and strength obtained from the numerical modelling were then compared with design requirements from BS EN 1993-1-8 and experimental data. The comparison showed not more than 35 % difference in strength and about 50 % difference in rotational stiffness between numerical modelling and experimental data. However, there was a noticeable difference between finite element models and analytical calculation. The differences were from 18 % to 66 % for strength and between 1 % and 145 % for stiffness. Finite element models showed a better agreement with experimental data as compared to analytical study. Edge stiffener of numerical model and theoretical stiffness calculation had caused significant difference in comparison.

Keywords: light gauge, steel connection, numerical modelling.

1. Introduction

Light gauge steel, also referred to as cold-formed steel, has been introduced to medium-rise construction in Industrial Building System (IBS) for a few decades. It is a popular reusable light gauge construction material with three methods of forming, namely cold-roll forming, press brake operation and bending brake operation [1].

In the construction industry, the validation of structural performance involves a range of procedures e.g. material analysis [2], dynamic analysis [3], monotonic action analysis, ultimate limit state analysis, serviceability limit state analysis, and etc. These procedures are important to obtain a quality and reliable structure. The second order effect of deformed frame in particular is an important factor in these analyses to check the stability of structures, which is in turn greatly dependent on the connections.

Connection consumes most of the fabrication cost in steelwork construction. Nevertheless, reduction in cost is still possible by adopting semi-rigid connection into the building design. In regard to this, the top-seat flange-cleat connection is one of the bolted joints capable of achieving semi-rigid connection behaviour [4]. In addition, this type of bolted connection has two prominent advantages: firstly, its installation procedures are simple and secondly, it requires no welding.

Research studies on the joints for light gauge steel design is still in low maturity. Moreover, during the design stage, design engineers are forced to refer to the design codes [5-6] for hot-rolled steel joint. The significant geometrical difference between hot-rolled and cold-formed steel often resulted in overdesigning the structure, causing the structures to fail at members rather than connecting components. This simply means that the local instability of cold-formed light gauge sections [7] has brought about the issue of inadequate design when the guidelines of hot-rolled design are adapted. Besides that, the research on joint behaviour for light gauge

sections that have been carried out so far [8-13] showed little contribution and the matter, in fact, has yet to be studied in-depth.

Monotonic and cyclic behaviour of top-seat flange-cleat connection was investigated by Luca [14] and the study had presented the modelling of this angle connection. A simplified method had also been suggested and implemented into code of practices [5]. Stiffness prediction by simple analytical procedure, shape parameter and ultimate moment had been obtained to contribute in power model of top-seat flange-cleat connection [15]. The power model was used to represent the moment-rotation curve of the connection. In order to simplify the complex semi-rigid calculation, new proposals on the calculation of the bending capacity in angle connection had been developed as well [16]. Distance between plastic hinges of top angle had been determined to calculate the flexural resistance of top-seat flange-cleat with web-cleat connection [16].

This paper, on the other hand, investigated the stiffness and strength behaviour of the top-seat flange-cleat connection in cold-formed double channel sections through the numerical modelling approach. Two types of connection were utilized, namely the 2 mm and 6 mm thick flange-cleat connections. The behaviour of the top-seat flange-cleat connections with different beam depths, ranging from 150 mm to 250 mm, namely DC150, DC200 and DC250 were also studied. Comparison among Eurocode 3 analytical models, finite element models and experimental data [17, 18] were carried out to predict the stiffness and strength behaviour.

2. Investigation Models

2. 1. Eurocode Model

According to BS EN 1993-1-8 [5], top-seat flange-cleat joint is considered as a moment connection. The stiffness of the joint is determined by its moment-rotation characteristic, where:

$$\varphi = \frac{M_{j,Sd}}{S_{j,ini}} \qquad \text{if } M_{j,Sd} < 2/3\ M_{j,Sd} \tag{1}$$

$$\varphi = M_{j,Sd} \times \frac{\left(\frac{1.5M_{j,Sd}}{M_{j,Rd}}\right)^{\psi}}{S_{j,ini}} \qquad \text{if } 2/3\ M_{j,Sd} < M_{j,Sd} < M_{j,Rd} \tag{2}$$

where $M_{j,Rd}$ is the design-resistant moment of the connection, $M_{j,Sd}$ is the moment applied, Ψ is 3.1 for bolted angle connection, and $S_{j,ini}$ is the initial stiffness of connection.

The calculation is obtained on the basis of component method introduced in Eurocode. The components are divided into tension and compression parts, namely bolt in tension; flange-cleat in bending; column flange in bending; column web in transverse tension; beam flange and web in compression; column flange compression; and column web in transverse compression. The $S_{j,ini}$ is obtained from the spring stiffness of each component where the $M_{j,Rd}$ is obtained from the yield line method of components.

2. 2. Experimental Investigation

The full-scaled isolated joint tests were carried out at the Laboratory of Structures and Materials, Universiti Teknologi Malaysia to identify the structural performance of light gauge steel top-seat flange-cleat connection under monotonic loading. The 2 mm thick light gauge cold-formed sections were assembled back-to-back to form an I-shape structural beam and

column. The 1.5 m I-beam was placed at 2 mm gap from the column flange and 1.5 m from the top of the column which was 3 m in length. The column and beam were connected with flange-cleats. The loading was applied at the distance of 1 m from the column flange onto the beam flange. The deflection was measured under the loading point and the rotations of beam and column were also measured as shown in Fig. 1.

The test was initialled with settlement of model when the loading was controlled to 10 % of the calculated maximum load and then released to zero setting. This whole process was completed to avoid ineffective load-carrying as it could affect the stiffness of the connection. The load was applied to the model under constant rate and the deflection and rotation were recorded for further analysis.

The experimental results had been recorded in previous researches [17, 18]. The load-deflection curves and moment-rotation curves were determined from the experimental results. The experimental testing in this study showed that the 2 mm cold-formed flange cleat yielded and the test ended due to excessive deformation. The 6 mm hot-rolled flange-cleat bent and failure occurred around the bolt area at the column flange.

Fig. 1. Experimental set up with planned data transducers system

2. 3. Finite Element Model

Finite element method was used as an alternative way to predict the structural behaviour to replace the tedious and costly experimental study. Basically, this numerical involved numerous mathematical calculations. The ABAQUS finite element code is the major code being used and this code primarily utilizes the stiffness method or displacement based finite element analysis. Referring to documentation [19], at equilibrium condition, written as a virtual work principle:

$$\int_V \sigma : \delta D dV = \int_S \boldsymbol{t}^T \cdot \delta v dS + \int_V \boldsymbol{f}^T \cdot \delta v dV \tag{3}$$

This virtual work statement has indicated that the rate of work done by the external forces subjected to any velocity field is equal to the rate of work done by the equilibrating stresses on the rate of deformation of the same virtual velocity field [19].

As for finite element interpolation, the general equation can be written as:

$$u = \boldsymbol{N}_N \boldsymbol{u}^N \tag{4}$$

where $\boldsymbol{N}_N$ are interpolation functions that rely on material coordinate system, $\boldsymbol{u}^N$ are nodal variables, and the summation convention is adopted for the uppercase subscripts and the nodal variables is used for the superscripts.

The units are fixed by the authors as such that length is in mm, force in N and stress in MPa (N/mm^2). Three-dimensional solid deformable elements (C3D20R, 20-node linear brick with reduced integration and hourglass control) were used in the ABAQUS/Standard static analysis. The top-seat flange-cleat connection in this research was geometrically symmetrical and the loading was in a single direction. Hence, only half of the connections were modelled to reduce the analysis time. The bolt threads were modelled as cylindrical shape with square bolt head and nut. These were also alternatives to save time as the bolts were not the critical parts in the analysis and by doing this, it would also minimize the contact frequency.

For interaction properties, the penalty friction formula and friction coefficient of 0.31 were applied to the tangential behaviour. Difference in friction coefficient will not give significant impact to the model [20]. Meanwhile, under normal condition, the penalty constraint enforcement method and "hard" contact were used. As for each contact, the type of interaction was surface-to-surface and included bolt head with beam, bolt thread with beam, bolt thread with flange-cleat, flange-cleat with beam, flange-cleat with column, nut with column, and bolt thread with column. Small sliding option was chosen in the analysis to fully transfer the loading to the supporting member.

The input values for section properties were taken from preliminary laboratory tests [17, 18]. Since there was no test data for bolt, elastic-perfectly-plastic behaviour was assigned as the material property to the model of bolt. Before the 10 mm global meshing size was assigned to the model, partitioning was applied to the model to give a structured brick element.

To perform nonlinear analysis in finite element method, all materials, boundaries and geometrical properties have to be assigned with nonlinearity condition to gain the nonlinear moment-rotation curve. Solving a single linear system will not result in a nonlinear analysis. Under specific loading, the nonlinear analysis has been found as a function of time and increased time to obtain nonlinear response [19]. The ABAQUS/Standard applies Newton's method to numerically calculate the solution of nonlinear equilibrium equations. This will primarily result in the convergence of Newton's method where after iteration i, an approximation $\boldsymbol{u}_i^M$, will be obtained and thus taken as the solution. By letting $\boldsymbol{u}_{i+1}^M$ to be the difference between this solution:

$$\boldsymbol{F}^N\left(\boldsymbol{u}_i^M + \boldsymbol{u}_{i+1}^M\right) = 0 \tag{5}$$

If $\boldsymbol{u}_i^M$ is a close approximation to the solution, the magnitude of each $\boldsymbol{u}_{i+1}^M$ will be small.

$$\boldsymbol{K}_i^{NP}\boldsymbol{c}_{i+1}^P = -\boldsymbol{F}_i^N \tag{6}$$

where:

$$\boldsymbol{K}_i^{NP} = \frac{\delta \boldsymbol{F}^N}{\delta \boldsymbol{u}^P}\left(\boldsymbol{u}_i^M\right) \tag{7}$$

is the Jacobian matrix and:

$$\boldsymbol{F}_i^N = \boldsymbol{F}^N\left(\boldsymbol{u}_i^M\right) \tag{8}$$

The next approximation to the solution is:

$$\boldsymbol{u}_{i+1}^{M} = \boldsymbol{u}_{i}^{M} + \boldsymbol{c}_{i+1}^{M} \tag{9}$$

and the iteration continues [19].

In order to save time and cost, Eq. 6 had been recalculated occasionally for the Jacobian matrix. Using this method, the Newton's method could converge quicker during the iteration process without neglecting the nonlinear properties in the iteration. The experimental works in this study showed that the top-seat flange-cleat connection deformed excessively. Thus, the Newton's method was used in the analysis to outline the formation of the large deformation by aborting the analysis that exceeded the accepted allowable deflection. With the above theoretical supports, the ABAQUS/Standard with Newton's method became the suitable analysis procedure for cold-formed top-seat flange-cleat connection.

3. Results and Discussion

Rotational stiffness is the crucial parameter to determine the moment-rotation behaviour of top-seat flange-cleat connection for light gauge steel construction. From Fig. 2, the graphs showed nonlinearity from static non-loading condition to gradually increased loading condition until the component collapsed. The nonlinearity was due to reduction in stiffness of the component. The rotational stiffness responded to the applied action, $K_j(F)$. Moment-rotation behaviour can be obtained from the function of joint rotational stiffness under various loading:

$$M_j = K_j \cdot \phi \tag{10}$$

The function started with no loading, which meant that there were no moment and rotation. Initially, the joint resistance was contributed by the elastic property of the material. The linear proportional relation between moment and rotation during this stage remained until the component experienced its first yield:

$$\frac{dM}{d\varphi} = K(F) \tag{11}$$

with $K(F) = K_e$, for $M \leq 2/3\ M_p$
$K(F) = K_p$, for $2/3\ M_p \leq M < M_p$
$K(F) = K_e / \alpha$, for $2/3\ M_p \leq M < M_p$

where K_e is the elastic rotational stiffness, K_p is the plastic rotational stiffness, and M_p is the plastic moment of the joint.

K_e remained constant within the elastic region before reaching two-third of M_p. As the loading increased, the joint entered the plastic zone, as indicated by the initiation of nonlinear behaviour. The stiffness gradually decreased and a nonlinearity curve developed from two-third of M_p to M_p. There are two phenomena after M_p; either failure will occur or the joint resistance will be replaced by strain hardening of the components. For cold-formed top-seat flange-cleat connection, experimental moment-rotation behaviour confirmed that the strain hardening phenomena prevailed. The elastic rotational stiffness in the moment-rotation graph reduced constantly until significant decrease of moment.

Stiffness and strength behaviour of top-seat flange-cleat joint can be represented using the moment-rotation curve. The comparison was fixed at 0.05 Rad [11] to determine the moment resistance. In order to increase the reliability of these finite element models, comparisons were also carried out at 0.03 Rad.

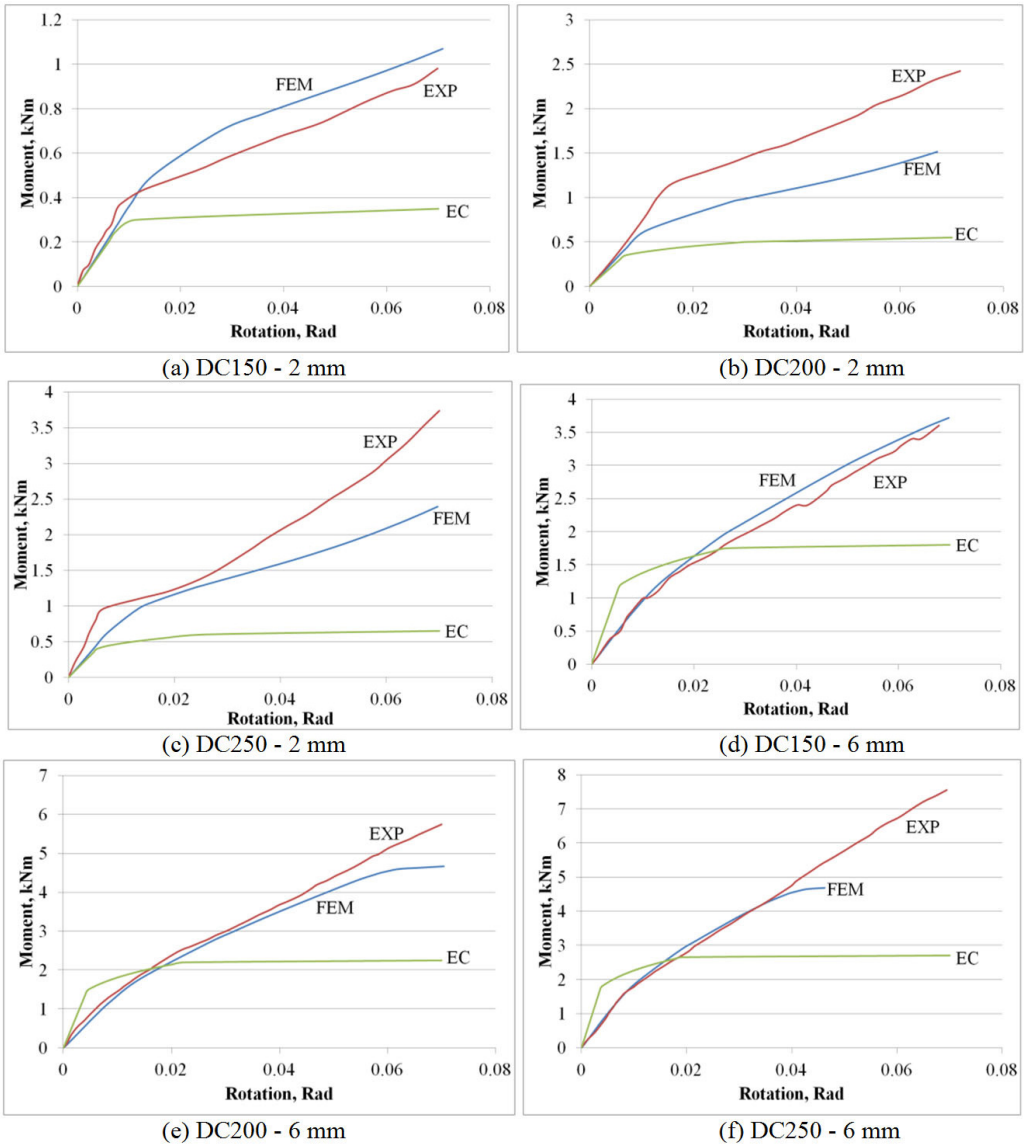

(a) DC150 - 2 mm (b) DC200 - 2 mm

(c) DC250 - 2 mm (d) DC150 - 6 mm

(e) DC200 - 6 mm (f) DC250 - 6 mm

Fig. 2. Moment rotation graphs of 2 mm and 6 mm flange-cleat

Table 1. Moment resistance of joint and difference in experimental, theoretical and finite element models at 0.03 Rad and 0.05 Rad

	$M_{j,0.03}$ (kNm/Rad)			Percentage difference			$M_{j,0.05}$ (kNm/Rad)			Percentage difference		
	EXP	EC	FEM	EC / EXP	FEM / EXP	EC / FEM	EXP	EC	FEM	EC / EXP	FEM / EXP	EC / FEM
DC150FC2	0.60	0.27	0.73	55%	22%	63%	0.78	0.30	0.88	62%	13%	66%
DC200FC2	1.48	0.52	0.99	65%	33%	47%	1.89	0.52	1.23	72%	35%	58%
DC250FC2	1.61	0.62	1.40	62%	13%	56%	2.56	0.62	1.83	76%	29%	66%
DC150FC6	2.00	1.78	2.17	11%	9%	18%	2.85	1.78	3.01	38%	6%	41%
DC200FC6	3.02	2.22	2.90	26%	4%	23%	4.43	2.22	4.04	50%	9%	45%
DC250FC6	3.83	2.66	3.91	31%	2%	32%	5.78	2.66	-	54%	-	-

Table 2. Initial and plastic rotational stiffness for experimental, Eurocode, and numerical models

	$S_{j,el}$ (kNm/Rad)			Percentage difference			$S_{j,pl}$ (kNm/Rad)			Percentage difference		
	EXP	EC	FEM	EC / EXP	FEM / EXP	EC / FEM	EXP	EC	FEM	EC / EXP	FEM / EXP	EC / FEM
DC150FC2	44.3	33.0	35.8	26%	19%	8%	9.9	8.8	8.9	11%	10%	1%
DC200FC2	73.9	52.0	61.0	30%	17%	15%	23.0	5.4	14.9	77%	35%	64%
DC250FC2	156.7	74.0	78.1	53%	50%	5%	20.1	8.2	20.9	59%	4%	61%
DC150FC6	97.6	219.0	93.4	124%	4%	134%	43.5	24.8	41.7	43%	4%	41%
DC200FC6	161.5	338.0	137.9	109%	15%	145%	68.4	39.2	60.0	43%	12%	35%
DC250FC6	44.3	33.0	35.8	26%	19%	8%	95.5	55.3	80.8	42%	15%	32%

The failure modes were carefully observed during the experimental investigation. For the 2 mm flange-cleat connection, the failure occurred due to the bending of top flange-cleat. The flange-cleat bended before the beam and column member failed. Yield line developed around the bolts of the column flange for the 6 mm hot-rolled flange-cleat connection. This failure was the same as shown in the finite element analysis.

The moment-rotation behaviour of finite element models, experiment works, and analytical prediction in Eurocode as depicted in Fig. 2 were similar. Meanwhile, the nonlinear moment-rotation curve obtained from all investigation models also indicated that these models would experience at least two rotational stiffnesses before collapsing. Nevertheless, the finite element, analytical and experimental analysis in this study exceeded 0.04 Rad before such condition happened. In comparison, Eurocode had the lowest values of $M_{j,0.03}$ and $M_{j,0.05}$ compared to those of finite element models and experimental investigation.

According to Table 1, the finite element models have a better agreement with experimental data in predicting the values of the joint resistance as compared to analytical models. The overall differences in joint capacity at 0.03 Rad and 0.05 Rad between experimental results and finite element analysis were not more than 35 %. For the 2 mm flange-cleat connection, the differences were between 13 % and 35 %. Meanwhile, for the 6 mm flange cleat connection, the differences were between 2 % and 9 %. The edge stiffener plays a major role in the bending of flange-cleat until failure. In the cold-rolling process, a single fold edge stiffener needs to sustain additional external action due to strain hardening. However, for the 6 mm flange-cleat connection, the bending of column flange until failure did not involve the edge zone, so the difference was small. For the 2 mm flange-cleat connection, the stiffness obtained from finite element models was lower than that of experimental data. The actual edge stiffener had increased the moment resistance of this light gauge steel connection.

With reference to Table 2, the finite element models obtained 17 % to 50 % and 4 % to 15 % differences with experimental results for initial rotational stiffness analysis of both 2 mm and 6 mm flange-cleat connection respectively. For plastic rotational stiffness, the differences for 2 mm and 6 mm flange-cleat connection were 4 % to 35 % and 4 % to 15 % respectively. As discussed earlier, edge stiffener was again the major player in the 2 mm flange-cleat connection.

In terms of strength and stiffness behaviour, the finite element models were 18 % to 66 % and 1 % to 145 % different respectively compared to those of Eurocode. Since the readings from Eurocode were significantly different from those of experimental data, the calculation of the design had to be validated by testing as described in BS EN 1993-1-3 [6].

Numerical models showed a close comparison with the experimental study than Eurocode theoretical calculation. From Fig. 2(d) to 2(f), for the 6 mm flange-cleat connection, the finite element models depicted a close relation with the experimental moment-rotation curve.

Calculation on the stiffness of flange-cleat under flexural behaviour was based on Eq. 12 [5]. Given the same angle, the determinate of stiffness value from Eq. 12 is the thickness, t_a. This, in fact, is the source of inadequacy in the calculated analytical value of stiffness. In this study, the cubic power showed an unfavourable increment in stiffness calculation. The lower power

calculation also showed a convergence results with the experimental data. Eurocode, then again, also showed a conservative design that excluded strain hardening in the plastic region:

$$k = \frac{0.9 l_{eff} t_a^3}{m^3} \tag{12}$$

where k is stiffness, l_{eff} is the effective length of equivalent T-stub, t_a is thickness of the angles, and m is the distance of bolt to edge corner.

From Fig. 2(a) to 2(c), the finite element models of 2 mm flange-cleat connection have a closer similarity with experimental data as compared to analytical calculation. Initially, all models showed a close relation in term of rotational stiffness, but the difference became obvious within the plastic region. The developed finite element models were calibrated with experimental data and thus showed a better agreement as compared to theoretical calculation.

4. Conclusions

Top-seat flange-cleat connection with cold-formed double channel sections was analysed using the finite element method. The 2 mm cold-formed brackets and 6 mm hot-rolled angles were utilized in the investigation. The results were compared with analytical and experimental results.

All investigation models (analytical, numerical and experimental models) showed multi-linear moment-rotation behaviour before collapse. Eurocode showed a conservative approach in determining the moment resistance of joints. Regarding the joint's moment resistance prediction at 0.03 Rad ($M_{j,0.03}$) and 0.05 Rad ($M_{j,0.05}$), the differences between finite element analysis and experimental investigation were not more than 35 %. For elastic rotational stiffness, the finite element models obtained 17 % to 50 % and 4 % to 15 % differences for the 2 mm and 6 mm flange-cleat connection respectively. Meanwhile, for plastic rotational stiffness, the differences were recorded at 4 % to 35 % for the 2 mm flange cleat connection and 4 % to 15 % for the 6 mm flange-cleat connection.

Edge stiffener contributed to the difference between finite element models and experimental data in the plastic region. Finite element models showed a difference between 18 % and 66 % in strength and between 1 % and 145 % in stiffness as compared to Eurocode. The significant difference in initial rotational stiffness between Eurocode model and experimental data was due to the cubic power of flange-cleat thickness in stiffness calculation.

The discrepancies of Eurocode and experimental study were from the theoretical stiffness calculation and conservative design under plastic behaviour. Cubic power of the flexural stiffness of flange-cleat had significantly stiffened the connection, this was recorded as lower value in the experimental results. Meanwhile, there was no strain hardening factor considered in the stiffness equation, this resulted in a more conservative behaviour in plastic region.

This research was limited to the 2 mm and 6 mm top-seat flange-cleat connection. For future study, the other factors such as the influence of edge stiffener and material imperfection should be included in the finite element analysis to obtain more reliable results that can represent the actual structural behaviour of full scale isolated joint test.

Acknowledgements

This research is funded by Universiti Teknologi Malaysia (Vot 01J09, 00J10 and 05J76). The authors gratefully acknowledge the supports from the Faculty of Civil Engineering, UTM and the Ministry of Higher Education of Malaysia (MOHE).

References

[1] **Wei-Wen Yu** Cold-Formed Steel Design. Third Edition, John Wiley & Sons, Inc., U. S., 2000.
[2] **J. Kwaśniewki, I. Dominik, K. Lalik** Application of self-oscillating system for stress measurement in metal. Journal of Vibroengineering, Vol. 14, Issue 1, 2012, p. 61-66.
[3] **I. Pakar, M. Bayat** Analytical study on the non-linear vibration of Euler-Bernoulli beams. Journal of Vibroengineering, Vol. 14, Issue 1, 2012, p. 216-224.
[4] **Pucinnotti Raffaele** Top-and-seat and web angle connections: prediction via mechanical model. Journal of Constructional Steel Research, Vol. 57, 2001, p. 661-694.
[5] British Standards Institution, Eurocode 3: Design of Steel Structures. Part 1.8: Design of Joints. U. K. BSI, BS EN 1993-1-8, 2005.
[6] British Standards Institution, Eurocode 3: Design of Steel Structures. Part 1.3: General Rules - Supplementary Rules for Cold-Formed Members and Sheeting. U. K. BSI, BS EN 1993-1-3, 2006.
[7] **Y. H. Lee, Y. L. Lee, C. S. Tan** Experimental investigation on cold-formed steel beams under pure bending. Jurnal Teknologi (Sciences & Engineering), Vol. 58, 2012, p. 13-20.
[8] **T. S. Kim, H. Kuwamura** Finite element modelling of bolted connections in thin-walled stainless steel plates under static shear. Thin-Walled Structures, Vol. 45, 2007, p. 407-421.
[9] **T. S. Kim, H. Kuwamura, T. J. Cho** A parametric study on ultimate strength of single shear bolted connection with curling. Thin-Walled Structures, Vol. 46, 2008, p. 38-53.
[10] **T. S. Kim, H. Kuwamura, S. H. Kim, Y. T. Lee, T. J. Cho** Investigation on ultimate strength of thin-walled steel single shear bolted connections with two bolts using finite element analysis. Thin-Walled Structures, Vol. 47, 2009, p. 1191-1202.
[11] **M. F. Wong, K. F. Chung** Structural behaviour of bolted moment connections in cold-formed steel beam-column sub-frames. Journal of Constructional Steel Research, Vol. 58, 2002, p. 253-274.
[12] **J. B. P. Lim, D. A. Nethercot** Ultimate strength of bolted moment-connections between cold-formed steel members. Thin-Walled Structures, Vol. 41, 2003, p. 1019-1039.
[13] **J. B. P. Lim, D. A. Nethercot** Stiffness prediction for bolted moment-connections between cold-formed steel members. Journal of Constructional Steel Research, Vol. 60, 2004, p. 85-107.
[14] **A. D. Luca** Behaviour and modelling of top & seat and top & seat and web angle connections. Connections in Steel Structures III, Elsevier, 1996, p. 289-298.
[15] **N. Kishi, W. F. Chen** Moment-rotation relations of semirigid connections with angles. Journal of Structural Engineering, Vol. 116, No. 7, 1990.
[16] **A. Loureiro, J. M. Reinosa, R. Gutiérrez, A. Moreno** New proposals on the calculation of the flexural resistance in angle connections. Journal of Constructional Steel Research, Vol. 67, 2011, p. 613-622.
[17] **C. S. Tan** Behaviour of Pin and Partial Strength Beam-to-Column Connection with Double Channel Cold-Formed Steel Sections. Ph. D. Thesis, Universiti Teknologi, Malaysia, 2009.
[18] **C. S. Tan, M. M. Tahir, P. N. Shek** Experimental investigation on angle cleat connections for cold-formed steel sections. Advanced in Steel and Aluminium Structures, Research Publishing, Singapore, 2011, p. 186-192.
[19] ABAQUS Analysis User's Manual. Version 6.7, 2007, ABAQUS Inc.
[20] **X. H. Dai, Y. C. Wang, C. G. Bailey** Numerical modelling of structural fire behaviour of restrained steel beam-column assemblies using typical joint types. Engineering Structures, Vol. 32, 2010, p. 2337-2351.